The 2009 IEEE/RSJ International Conference on
Intelligent Robots and Systems
October 11-15, 2009 St. Louis, USA

Pinching 2D Object with Arbitrary Shape by Two Robot Fingers under Rolling Constraints

Morio Yoshida, Suguru Arimoto, and Kenji Tahara

Abstract— **Modeling of pinching an object with arbitrary shape by a pair of robot fingers with hemispherical ends in a horizontal plane is proposed in a mathematical and computational manner. Since the curvature of an object contour with an arbitrary curve is variable according to the change of the contact point between the object surface and the rigid finger tip, the arclength paremeter "s" explicitly appears in the overall fingers-object dynamics. It is shown that the overall fingers-object system should be accompanied with the first-order differential equation of the parameter "s" that includes the curvatures of both the object contour and finger-tip curve. A control input, which is of the same category as the control input called "blind grasping" appeared in our former papers, is utilized for the realization of stable grasp. The control input does neither need to use the kinematic information of the object nor use any external sensing. Finally, numerical simulations are carried out in order to confirm the effectiveness of our proposed model and control input.**

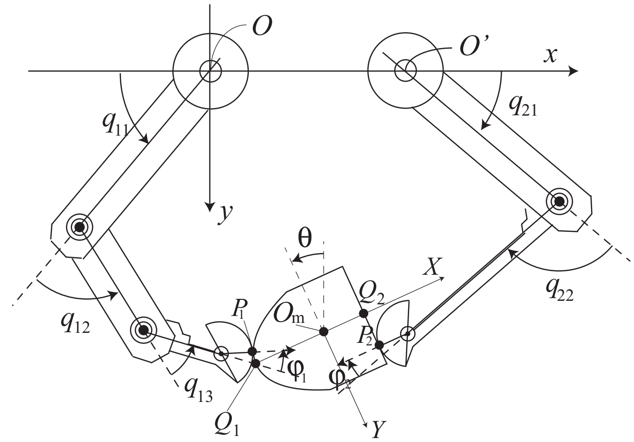

Fig. 1. A pair of robot fingers pinching an object with arbitrary shape

I. INTRODUCTION

The fact that humans easily and smoothly manipulate many kinds of objects has attracted many people since the motion of this movement includes the intriguing properties; finger-thumb opposition, redundancy of finger joints, arbitrary shape of a finger tip or a pinched object, and soft and rolling contact between a finger tip and an object surface.

These properties are beneficial and effective to realize the robots used in daily life, and robotic researchers have devoted their time to analyze, simulate, and create the finger robots with these properties [1] [2] [3]. Most of explorations in robotics, however, remain in kinematics or motion planning for the realization of force-torque closure to accomplish stable grasp. The rolling geometry between two surfaces of arbitrary shape was discussed in detail [4] [5]. This research focused on semi-dynamic or kinematic approaches and did not show any explicit forms representing the physical interaction between two bodies in the wrench space. Researchers in multibody dynamics propose many models in a dynamic sense but do not consider rolling contact in our sense [6] [7]. They have missed an important aspect of physical interaction between two bodies under rolling constraints in a dynamic sense, despite the strong demand for unveiling the correlated mechanism to realize interactive robots with human movements.

Arimoto *et al.* [8], around 2000, proposed the 2-D dynamic pinching model by a pair of robot fingers with hemispherical ends under rolling constraints, by the aid of the assumption that the velocity of the finger tip in the tangent direction must be equal to the velocity on the object surface when the shape of the pinched object is limited to flat surfaces. This model was extended in 2006 to a three dimensional model [9]. A mathematical model was derived, as a set of equations of motion of the fingers-object system under Pfaffian constraints due to rolling constraints, and the equations representing infinitesimal rotations of the object. The control input called "blind grasping", which need not use object information or external sensing, comfirms stable grasping. Because of the lack of the total number of wrench vectors on the object, spinning motion arises around the opposing axis by two contact points between finger tips and object surfaces. This proposed model has six wrench vectors on the object but seven wrench vectors are needed to satisfy force/torque balance in a three dimensional case. A physically faithful viscosity model [10] was introduced to blunt the spinning motion. However, all models proposed by Arimoto *et al.* [9] were restricted to the flat surfaces.

In this paper, a new model of pinching an object with arbitrary shape by a pair of robot fingers with hemispherical ends in a horizontal plane is proposed in a mathematical and computational manner (see Fig.1). A control input for realizing stable grasping, which is of the same category of the control input called "blind grasping", is proposed. In

This work was partially supported by Japan Society for the Promotion of Science (JSPS), Grant-in-Aid for Scientific Research (B) (20360117).

M. Yoshida, S. Arimoto, and K. Tahara are with the RIKEN-TRI-Collaboration Center for Human-Interactive Robot Research, RIKEN, Nagoya, Aichi, 463-0003, Japan yoshida@nagoya.riken.jp

S. Arimoto is with the Department of Robotics, Ritsumeikan University, Kusatsu, Shiga, 525-8577, Japan arimoto@fc.ritsumei.ac.jp

K. Tahara is with the Organization for the Promotion of Advanced Research, Kyushu University, Fukuoka, 819-0395, Japan tahara@ieee.org

the case of rolling contacts with an object with arbitrary shape, its contour curvature varies according to the change of the contact and then the arclength parameter “s” must be taken into account to describe movement of the contact point along the object’s contour curve. The overall fingers-object system is shown to be governed by Euler-Lagrange’s equations parametrized by the arclength parameter and at the same time the first order differential equation of the parameter “s” is derived. It is noted that Lagrange’s equations representing the overall fingers-object system and the update equation of “s” should be solved simultaneously so that they satisfy the principle of causality. Finally, numerical simulator is constructed based upon our proposed model, and by applying our proposed control signals, numerical simulations are carried out for validating of the model and the effectiveness of the control inputs.

II. Dynamics

Modeling of pinching a rigid object with arbitrary shape by two robot fingers with 3 DOFs and 2 DOFs is schematically shown in Fig.1. In the coordinate system, numerical values of all angles are positive in counterclockwise direction. The finger tips of two robot fingers are of hemispherical shape and rigid. We introduce the local coordinate O_m-XY fixed at the object frame, and define unit vectors $\boldsymbol{r}_X$ on the X axis and $\boldsymbol{r}_Y$ on the Y axis (see Fig.2). The left-side contour of the object is expressed by a curve attached to the local coordinate $(X(s_1), Y(s_1))$ (see Fig.3), and similarly the right-side contour by a curve with the local coordinate $(X(s_2), Y(s_2))$ (see Fig.4), with the aid of arclength parameters $s_i (i = 1, 2)$. P_1 is the contact point between the finger tip and the object surface, $\boldsymbol{b}_1$ the tangent unit vector of both the finger tip and the contour of the object at contact point P_1, and $\boldsymbol{n}_1$ the normal unit vector to the tangent vector $\boldsymbol{b}_1$. The angle between the normal unit vector $\boldsymbol{n}_1$ and the X axis is denoted by θ_1, and is determined as follows:

$$\theta_1(s_1) = \mathrm{arct}\left(X'(s_1)/Y'(s_1)\right) \tag{1}$$

where $X'(s_1) = \mathrm{d}X(s_1)/\mathrm{d}s_1$ and $Y'(s_1) = \mathrm{d}Y(s_1)/\mathrm{d}s_1$. Similarly θ_2 (see Fig.4) is determined as follows:

$$\theta_2(s_2) = \mathrm{arct}\left(X'(s_2)/Y'(s_2)\right) \tag{2}$$

where $X'(s_2) = \mathrm{d}X(s_2)/\mathrm{d}s_1$ and $Y'(s_2) = \mathrm{d}Y(s_2)/\mathrm{d}s_2$. $\overline{P_1P_1'}$ is expressed in the local coordinate $(X(s_1), Y(s_1))$ as follows:

$$\overline{P_1P_1'} = l_{n1}(s_1) = -X(s_1)\cos\theta_1(s_1) + Y(s_1)\sin\theta_1(s_1) \tag{3}$$

On the other hand, $\overline{P_1P_1'}$ is represented in the inertia frame O-xy as follows:

$$\begin{aligned}\overline{P_1P_1'} \;&=\; (x - x_{01})\cos(\theta + \theta_1)\\ &\quad -(y - y_{01})\sin(\theta + \theta_1(s_1)) - r_1\end{aligned} \tag{4}$$

Then, the contact constraint of the left side of the object is derived as the holonomic constraint:

$$\begin{aligned}Q_1 \;&=\; -(x - x_{01})\cos(\theta + \theta_1(s_1))\\ &\quad -(y - y_{01})\sin(\theta + \theta_1(s_1))\\ &=\; -(r_1 + l_{n1}(s))\end{aligned} \tag{5}$$

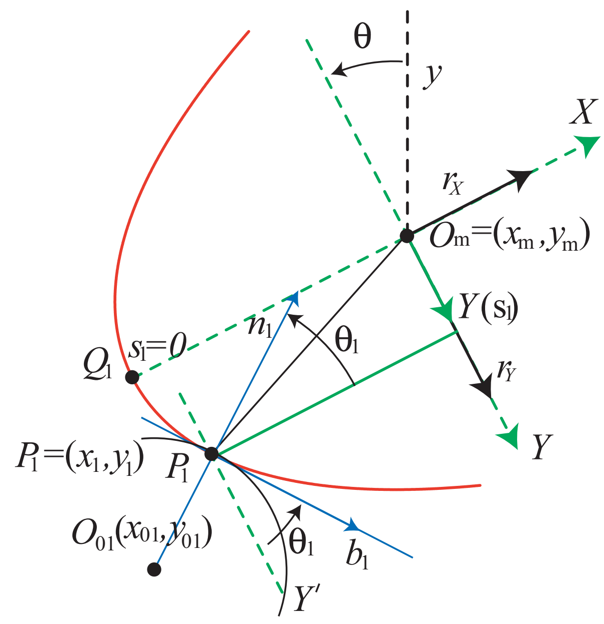

Fig. 2. Relationship between local coordinate O-XY and fingertip O_{01}

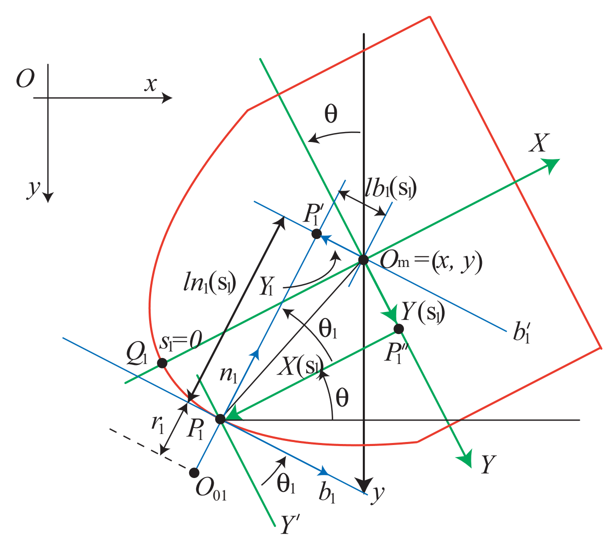

Fig. 3. Geometrical relationship based on length parameter “s_1”

Similarly the contact constraint of the right side of the object is derived as follows:

$$\begin{aligned}Q_2 \;&=\; (x - x_{02})\cos(\theta + \theta_2(s_2))\\ &\quad -(y - y_{02}\sin(\theta + \theta_2(s_2)))\\ &=\; -(r_2 + l_{n2}(s_2))\end{aligned} \tag{6}$$

where

$$l_{n2}(s_2) \;=\; X(s_2)\cos\theta_2(s_2) - Y(s_2)\sin\theta_2(s_2) \tag{7}$$

$\overline{O_mP_1'}$ is expressed in the local coordinate $(X(s_1), Y(s_1))$ as follows:

$$\overline{O_mP_1'} = l_{b1}(s_1) = X(s_1)\sin\theta_1 + Y(s_1)\cos\theta_1 \tag{8}$$

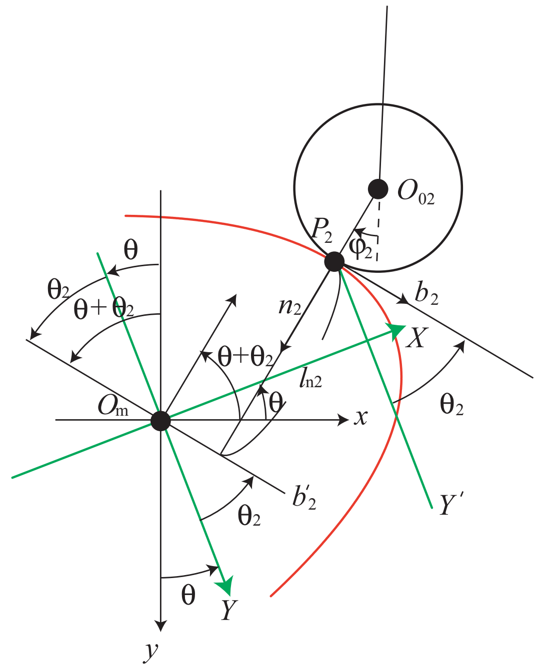

Fig. 4. Geometrical relationship of the right side of an object

On the other hand, $\overline{O_m P_1'}$ is represented in the inertia frame as follows:

$$\begin{aligned} R_1(t) &= -(x - x_{01})\sin(\theta+\theta_1) \\ &\quad -(y-y_{01})\cos(\theta+\theta_1) = l_{b1}(s_1) \end{aligned} \tag{9}$$

Rolling contact means that the robot finger tip rolls on the object surface without slipping. In other words, the object's velocity along vector $\boldsymbol{b}_1$ at contact point P_1 must be equal to the finger tip's velocity along vector $\boldsymbol{b}_1$ at the point, at instant t, as follows:

$$r_1 \frac{\partial \phi_1}{\partial t} + \frac{\partial}{\partial t} R_1(t) = 0 \tag{10}$$

where φ_1 is defined as follows (see Fig.1):

$$\begin{aligned} \varphi_1 &= \pi + (\theta+\theta_1) - (q_{11}+q_{12}+q_{13}) \\ &= \pi + (\theta+\theta_1) - p_1 \end{aligned} \tag{11}$$

where $p_1 = q_{11} + q_{12} + q_{13}$. Eq.(10) can fortunately be integrated in the sense of Frobenius (see [11]). In fact, we define

$$\overline{R_1}(t, s_1) = r_1\{\theta + \theta_1(s_1) - p_1\} + s_1 + R_1 - l_{b1}(s_1) \tag{12}$$

and see that $\partial \overline{R_1}(t,s_1)/\partial t = 0$ is reduced to eq.(10). It is found out that (see [11])

$$\frac{\mathrm{d}\overline{R_1}}{\mathrm{d}t} = \frac{\partial \overline{R_1}}{\partial t} + \frac{\partial \overline{R_1}}{\partial s_1}\frac{\mathrm{d}s_1}{\mathrm{d}t} = 0 \tag{13}$$

It is possible to define

$$\tilde{R}_1 = \overline{R_1}(t, s_1(t)) - \overline{R_1}(0, s_1(0)) \tag{14}$$

Similarly the rolling constraint at the right hand finger is derived as follows:

$$r_2 \frac{\partial \phi_2}{\partial t} + \frac{\partial}{\partial t} R_2(t) = 0 \tag{15}$$

where

$$\begin{aligned} R_2(t) &= -(x - x_{02})\sin(\theta+\theta_2(s_2)) \\ &\quad -(y-y_{02})\cos(\theta+\theta_2(s_2)) = l_{b2}(s_2) \end{aligned} \tag{16}$$

$$l_{b2}(s_2) = X(s_2)\sin\theta_2(s_2) + Y(s_2)\cos\theta_2 \tag{17}$$

$$\begin{aligned} \varphi_2 &= -\pi + (\theta+\theta_2) - (q_{21}+q_{22}) \\ &= -\pi + (\theta+\theta_2) - p_2 \end{aligned} \tag{18}$$

and $p_2 = q_{21} + q_{22}$. Since eq.(15) can be integrated as discussed in eq.(10) (see [11]), we similarly define

$$\tilde{R}_2 = \overline{R_2}(t, s_2(t)) - \overline{R_2}(0, s_2(0)) \tag{19}$$

where

$$\overline{R_2}(t, s_2) = -r_2\{\theta + \theta_2(s_2) - p_2\} + s_2 + R_2 - l_{b2}(s_2) \tag{20}$$

and $\partial \overline{R_2}(t,s_2)/\partial t = 0$ leads to eq.(15). The following equation can be confirmed (see [11])

$$\frac{\mathrm{d}\overline{R_2}}{\mathrm{d}t} = \frac{\partial \overline{R_2}}{\partial t} + \frac{\partial \overline{R_2}}{\partial s_2}\frac{\mathrm{d}s_2}{\mathrm{d}t} = 0 \tag{21}$$

Eq.(9) is reduced to the constraint form in terms of infinitesimally small variation:

$$\begin{aligned} &\big(J_1^{\mathrm{T}}(q_1)\boldsymbol{b}_1(\theta) - r_1\boldsymbol{e}_1, -\sin(\theta+\theta_1), \\ &\quad -\cos(\theta+\theta_1), -l_{n1}\big)\,(\boldsymbol{dq}_1, \mathrm{d}x, \mathrm{d}y, \mathrm{d}\theta)^{\mathrm{T}} = 0 \end{aligned} \tag{22}$$

where $\boldsymbol{b}_1(\theta)=(\sin(\theta+\theta_1), \cos(\theta+\theta_1))^{\mathrm{T}}$,$\boldsymbol{dq}_1=(\mathrm{d}q_{11},\mathrm{d}q_{12},\mathrm{d}q_{13})^{\mathrm{T}}$, $J_1=\partial(x_{01},y_{01})/\partial(q_{11},q_{12},q_{13})$, and $\boldsymbol{e}_1=(1,1,1)^{\mathrm{T}}$. Similarly, eq.(12) is reduced to

$$\begin{aligned} &\big(J_2^{\mathrm{T}}(q_2)\boldsymbol{b}_2(\theta) + r_2\boldsymbol{e}_2, -\sin(\theta+\theta_2), \\ &\quad -\cos(\theta+\theta_2), l_{n2}\big)\,(\boldsymbol{dq}_2, \mathrm{d}x, \mathrm{d}y, \mathrm{d}\theta)^{\mathrm{T}} = 0 \end{aligned} \tag{23}$$

where $\boldsymbol{b}_2(\theta)=(\sin(\theta+\theta_2), \cos(\theta+\theta_2))^{\mathrm{T}}$,$\boldsymbol{dq}_2=(\mathrm{d}q_{21},\mathrm{d}q_{22})^{\mathrm{T}}$, $J_2=\partial(x_{02},y_{02})/\partial(q_{21},q_{22})$, and $\boldsymbol{e}_2=(1,1)^{\mathrm{T}}$.

By associating Lagrange's multipliers f_i with the constraints $Q_i = 0$ $(i=1,2)$(eqs.(5) and (6)), we define a Lagrangian:

$$\begin{aligned} L &= \sum_{i=1,2}\frac{1}{2}\dot{q}_i^{\mathrm{T}} G_i(q_i)\dot{\boldsymbol{q}}_i + \frac{1}{2}M(\dot{x}^2+\dot{y}^2) \\ &\quad + \frac{1}{2}I\dot{\theta}^2 - f_1Q_1 - f_2Q_2 \end{aligned} \tag{24}$$

where $\boldsymbol{q}_1 = (q_{11}, q_{12}, q_{13})^{\mathrm{T}}$,$\boldsymbol{q}_2 = (q_{21}, q_{22})^{\mathrm{T}}$,$G_i(q_i)$ denotes the inertia matrix for finger i $(i = 1,2)$, M and I denote the mass and inertia moment of the object. Due to utilizing the Lagrangian and associateing Lagrange's multipliers λ_i with eqs.(22) and (23), the dynamic equations of the overall fingers-object system are derived as follows:

$$\begin{aligned} &I\ddot{\theta} - f_1 l_{b1}(s_1) + f_2 l_{b2}(s_2) \\ &\quad -\lambda_1 l_{n1}(s_1) + \lambda_2 l_{n2}(s_2) = 0 \end{aligned} \tag{25}$$

$$M\ddot{x} - f_1\cos(\theta+\theta_1) + f_2\cos(\theta+\theta_2) \\ -\lambda_1\sin(\theta+\theta_1) - \lambda_2\sin(\theta+\theta_2) = 0 \quad (26)$$

$$M\ddot{y} + f_1\sin(\theta+\theta_1) - f_2\sin(\theta+\theta_2) \\ -\lambda_1\cos(\theta+\theta_1) - \lambda_2\cos(\theta+\theta_2) = 0 \quad (27)$$

$$G_1(q_1)\ddot{q}_1 + \left\{\frac{1}{2}\dot{G}_1 + S_1\right\}\dot{q}_1 + f_1 J_1^{\mathrm{T}}(q_1)\boldsymbol{n}_1(\theta) \\ +\lambda_1\left\{J_1^{\mathrm{T}}(q_1)\boldsymbol{b}_1(\theta) - r_1\boldsymbol{e}_1\right\} = u_1 \quad (28)$$

$$G_2(q_2)\ddot{q}_2 + \left\{\frac{1}{2}\dot{G}_2 + S_2\right\}\dot{q}_2 + f_2 J_2^{\mathrm{T}}(q_2)\boldsymbol{n}_2(\theta) \\ +\lambda_2\left\{J_2^{\mathrm{T}}(q_2)\boldsymbol{b}_2(\theta) + r_2\boldsymbol{e}_2\right\} = u_2 \quad (29)$$

where

$$\boldsymbol{n}_1(\theta) = \begin{pmatrix}\cos(\theta+\theta_1)\\ -\sin(\theta+\theta_1)\end{pmatrix}, \boldsymbol{n}_2(\theta) = \begin{pmatrix}-\cos(\theta+\theta_2)\\ \sin(\theta+\theta_2)\end{pmatrix}, \quad (30)$$

and $u_i(i=1,2)$ stand for control inputs.

Since the arclength parameters $s_i(i=1,2)$ depend on the time parameter t, the parameters $s_i(i=1,2)$ should be updated as follows:

$$\frac{\mathrm{d}s_i}{\mathrm{d}t} = \frac{r_i}{1+r_i\kappa_i(s_i)}(\dot{p}_i - \dot{\theta}), i = 1,2 \quad (31)$$

where $\kappa_i(s_i)(i=1,2)$ denote the curvature of the object contours at contacts as follows:

$$\kappa_i(s_i) = X''(s_i)Y'(s_i) - X'(s_i)Y'(s_i), \quad i=1,2 \quad (32)$$

It is interesting to note that the curvatures $\kappa_i(s_i)(i=1,2)$ of the object contours appear in the update equations (eq.(31)) but not in the overall Lagrange's equations (eqs.(25) $\sim$ (29)).

III. Control Signal

Since a family of control inputs called "blind grasping" [9] neither need use the kinematic information of the object nor any external sensing, that is, we do not need to consider the shape of the object, we can apply the concept of our previous control input [9] to this stabilization problem of grasping of the object with arbitrary shape. Therefore a control input, realizing stable grasping with an object with arbitrary shape, is proposed as follows:

$$u_i = -c_i\dot{q}_i + (-1)^i\frac{f_d}{r_1+r_2}J_i^{\mathrm{T}}(q_i)\begin{pmatrix}x_{01}-x_{02}\\ y_{01}-y_{02}\end{pmatrix} \\ -r_i\hat{N}_i\boldsymbol{e}_i, \qquad i=1,2 \quad (33)$$

where

$$\hat{N}_i(t) = \gamma_i^{-1}r_i\left(p_i(t) - p_i(0)\right), \qquad i=1,2, \quad (34)$$

γ_i and $c_i(i=1,2)$ are positive constants, and $p_i(0)$ initial values of $p_i(t)$. The first term of the right hand side of eq.(33) plays a role of damping. The second term is a signal based upon the opposable force between O_{01} and O_{02}. The third term compensates the difference among initial poses of the overall system.

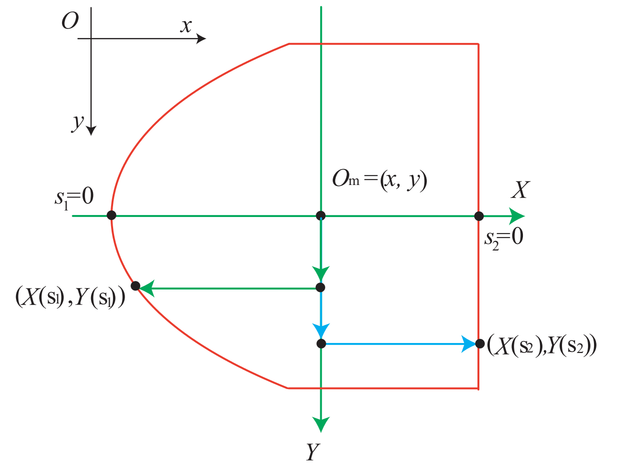

Fig. 5. Local Coordinates $(X(s_i), Y(s_i)),(i=1,2)$ used in the simulation

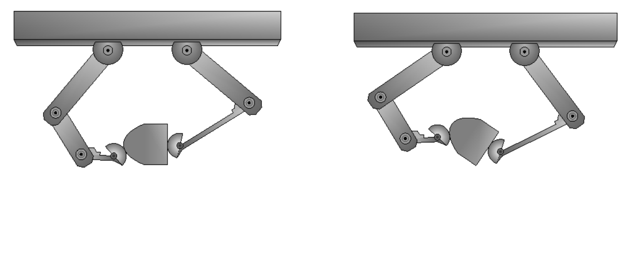

(a) Initial pose (b) After 5 seconds

Fig. 6. Motion of pinching a 2-D object with arbitrary shape

IV. Numerical Simulation

We construct a numerical simulator based on our proposed model and physical parameters of the fingers-object system given in Table I. Numerical simulations are carried out by applying our proposed control inputs (eq.(33)) using the parameters of control gains given in Table II and the initial

TABLE I

Physical parameters of the fingers and object.

$l_{11}=l_{21}=l_{22}$	length	0.065 [m]
l_{12}	length	0.039 [m]
l_{13}	length	0.026 [m]
m_{11}	weight	0.045 [kg]
m_{12}	weight	0.025 [kg]
m_{13}	weight	0.015 [kg]
m_{21}	weight	0.045 [kg]
m_{22}	weight	0.040 [kg]
r_0	link radius	0.005 [m]
$r_i(i=1,2)$	radius	0.010 [m]
L	base length	0.063 [m]
M	object weight	0.040 [kg]

TABLE II

Parameters of control signals.

f_d	internal force	1.000 [N]
c	damping coefficient	0.006 [Nms]
$\gamma_i(i=1,2)$	regressor gain	0.001 [s^2/kg]

TABLE III

INITIAL VALUES

$q_{11}(0)$	initial angle	$5.000 \times \pi/18$[rad]
$q_{12}(0)$	initial angle	$7.168 \times \pi/18$[rad]
$q_{13}(0)$	initial angle	$5.545 \times \pi/18$[rad]
$q_{21}(0)$	initial angle	$-4.008 \times \pi/18$[rad]
$q_{22}(0)$	initial angle	$-10.82 \times \pi/18$[rad]
$\theta(0)$	initial angle	$0.000 \times \pi/18$[rad]
$x(0)$	initial point	3.243×10^2[m]
$y(0)$	initial point	7.500×10^2[m]
$s_1(0)$	internal arclength parameter	0.005 [m]
$s_2(0)$	internal arclength parameter	0.001 [m]

values given in Table III in order to confirm the stability of motion of the overall fingers-object system (eqs.(25) $\sim$ (29)). The curves $c(s_i)$,$(i = 1, 2)$ with local coordinates $(X(s_i), Y(s_i))$ are used in the simulations as follows (see Fig.5):

$$X(s_1) = -0.03 + \frac{\sqrt{1 + 4 \times 50^2 \times s_1^2}}{2 \times 50} \text{ [m]} \quad (35)$$

$$Y(s_1) = \frac{\text{Asinh}(2 \times 50 \times s_1)}{2 \times 50} \text{ [m]} \quad (36)$$

$$X(s_2) = 0.015 \text{ [m]} \quad (37)$$

$$Y(s_2) = s_2 \text{ [m]} \quad (38)$$

It is noted that, since the $s_i(i = 1, 2)$ are arclength parameters, $\sqrt{X'(s_i)^2 + Y'(s_i)^2} = 1$,$(i = 1, 2)$. In the case, since the object contour in the right side is flat, the curvature $\kappa_2(s_2)$ becomes zero. Their initial values must be determined to satisfy the rolling and contact conditions (eqs.(5),(6),(12) and (20)), in order to carry out the simulations. The constraint stabilization method (CSM) [12] can be used to maintain the rolling and contact constraints. The motion obtained by the simulation is depicted in Fig.6. Figs.8 $\sim$ 11 and 16 $\sim$ 20 show that all velocities of the dynamic equations (eqs.(25) $\sim$ (29)) converge to zero, and that all Lagrange's multipliers converge to some constant values. These results show that motion of the overall fingers-object dynamics converges to some equilibrium state, and stable grasping is eventually realized from the viewpoint of numerical simulation.

V. CONCLUSION

In this paper, a 2-D pinching model by two robot fingers of an object is derived mathematically and tested numerically to ensure whether the model works with physical reality. Since the curvature of the object contour is variable according to the change of the contact point between the object surface and the rigid finger tip, the arclength paremeter "s" is taken into account to describe motion of the overall fingers-object system. The overall fingers-object system should be accompanied with the first-order differential equation of the arclength parameter "s". The dynamical equations that generate motion of the overall fingers-object system and the update equations of arclength parameters should be numerically integrated simultaneously so that they satisfy the principle of causality. It is shown that the proposed control input called

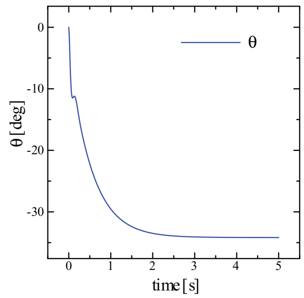

Fig. 7. Trajectory of object angle θ

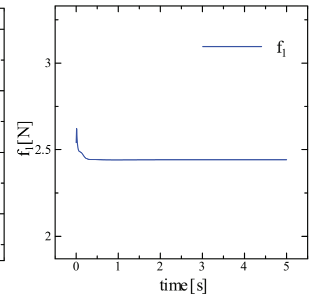

Fig. 8. Trajectory of normal force f_1

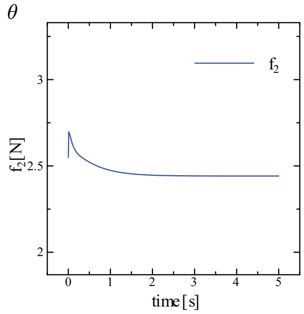

Fig. 9. Trajectory of normal force f_2

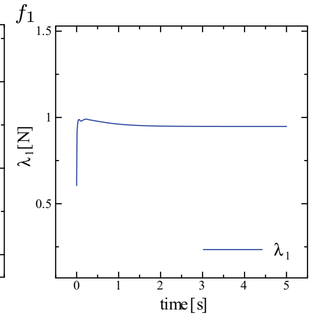

Fig. 10. Trajectory of tangential force λ_1

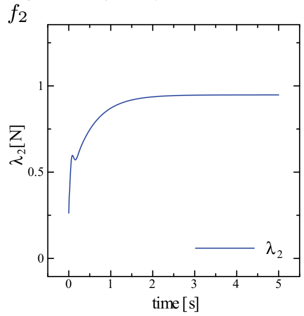

Fig. 11. Trajectory of tangential force λ_2

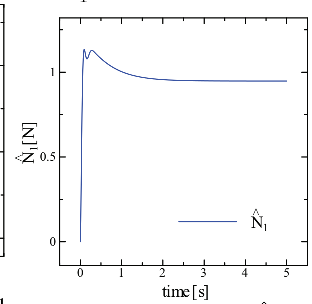

Fig. 12. Trajectory of $\hat{N}_1$

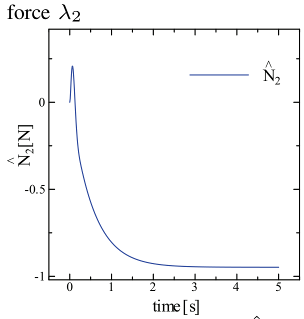

Fig. 13. Trajectory of $\hat{N}_2$

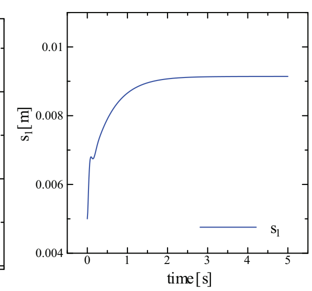

Fig. 14. Trajectory of arclength parameter s_1

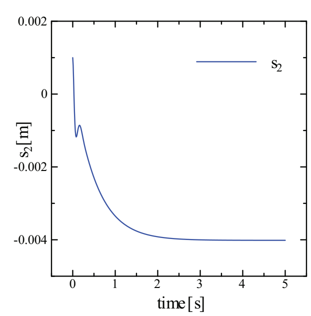

Fig. 15. Trajectory of arclength parameter s_2

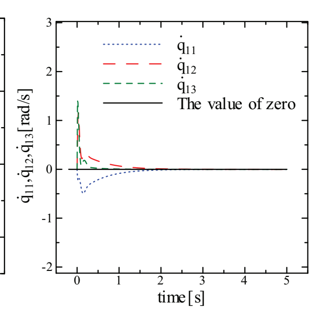

Fig. 16. Trajectories of angular velocities $\dot{q}_{11}$,$\dot{q}_{12}$ and $\dot{q}_{13}$

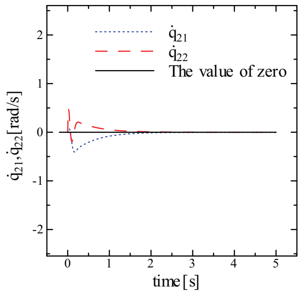

Fig. 17. Trajectories of angular velocities $\dot{q}_{21}$ and $\dot{q}_{22}$

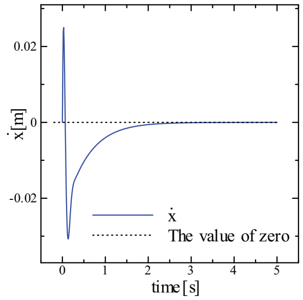

Fig. 18. Trajectory of translational velocity $\dot{x}$

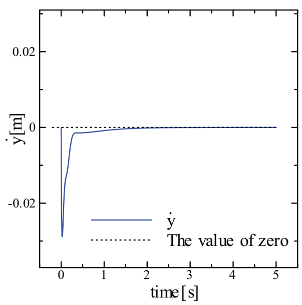

Fig. 19. Trajectory of translational velocity $\dot{y}$

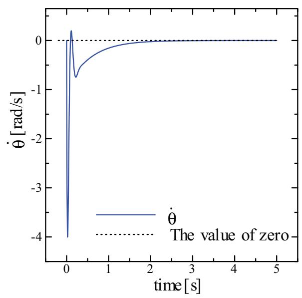

Fig. 20. Trajectory of rotational velocity $\dot{\theta}$

"blind grasping" is effective in realizing stable grasping as far as numerical simulations are concerned. The problem of stability of control inputs for our proposed pinching model will be tackled more in detail from numerical simulation and at the same time from the mathematical analysis in a near future.

VI. ACKNOWLEDGMENTS

This work was partially supported by Japan Society for the Promotion of Science (JSPS), Grant-in-Aid for Scientific Research (B) (20360117).

REFERENCES

[1] R. M. Murray, Z. Li, and S. S. Sastry, *A Mathematical Introduction to Robotic Manipulation*, CRC Press, Boca Raton,FL, USA and Tokyo, Japan, 1994.

[2] M. R.Cutkovsky, *Robotic Grasping and Fine Manipulation*, Kluwer Academic, Dordrecht, Netherlands, 1985.

[3] A. Bicchi. Hands for dexterous manipulation and robust grasping: A difficult road toward simplicity, *IEEE Trans. on Robotics and Automation*, Vol.16, pp.652–662, 2000.

[4] D.J. Montana. The kinematics of contact and grasp, *Int. J.of Robotics Research*, Vol.7, No.3, pp.17-32, 1988.

[5] D.J. Montana, "Contact stability for two-fingered grasps", *IEEE Trans. on Robotics and Automation*, vol.8, no.4, pp.421-430,1992.

[6] T. R. Kane *Dynamics*. Holt, Rinehart and Winston, Inc, New York, 1968.

[7] A.A. Shabana, *Computational Dynamics, Second Edition*, Wiley-Interscience, New York, USA, 2001.

[8] S. Arimoto, P.T.A. Nguyen, H.-Y. Han, and Z. Doulgeri. Dynamics and control of a set of dual fingers with soft tips, *Robotica*, Vol.18, No.11, pp.71-80, 2000.

[9] S. Arimoto *Control Theory of Multi-fingered Hands*, Springer-Verlag, London, 2008.

[10] M. Yoshida, S. Arimoto, and K. Tahara. Modeling and Control of a Pair of Robot Fingers under the Orderless Actuations at Saddle Joint, *Proc. of the 2009 IEEE Robotics and Automation*, pp.2499-2505, Kobe, Japan, May 12-17, 2009.

[11] S. Arimoto, "Dexterity and Control of Robot Arms and Hands: A Riemannian Geometry Approach", *IEICE Fundamentals Review*, Vol.2, No.4, pp.1-11, 2009.

[12] J. Baumgarte, "Stabilization of constraint and integrals of motion in dynamical systems", *Comput. Methods in Appl. Mech. and Eng.*, Vol.1, No.1, pp.1–16, 1972.